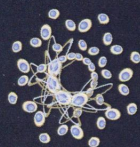
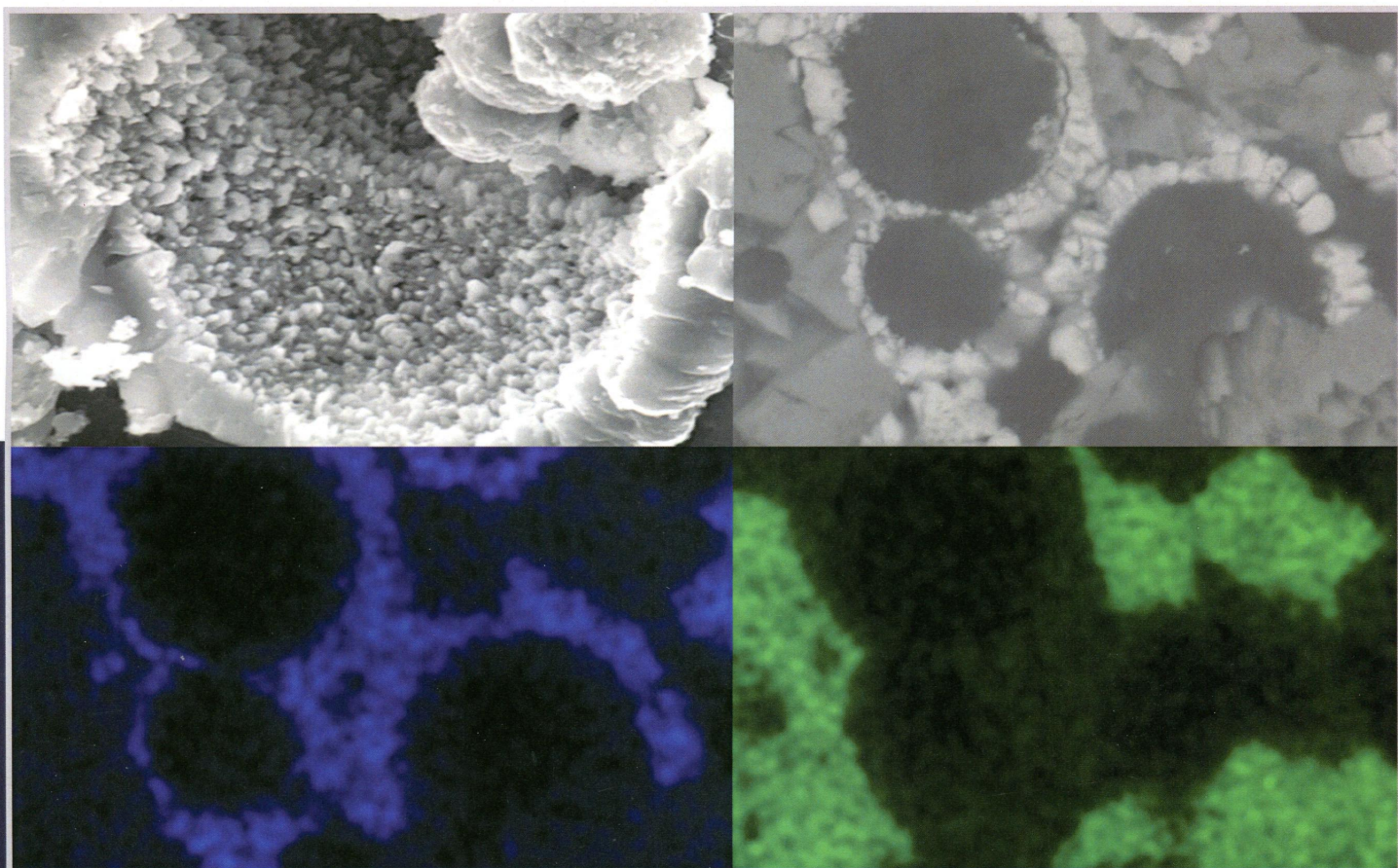


# JOURNAL OF NUCLEAR MATERIALS

[www.elsevier.com/locate/jnucmat](http://www.elsevier.com/locate/jnucmat)

NOVEMBER 2014 | ISSN 0022-3115 | VOLUME 454 (2014) ISSUES 1-3



Organisers of NuMat  
conference series

## EDITORS

**L.K. MANSUR (Chairman)**  
Oak Ridge, TN, USA

**T. MUROGA**  
Toki, Japan

**R.E. STOLLER**  
Oak Ridge, TN, USA

**M. GRIFFITHS**  
Chalk River, ON, Canada

**T. OGAWA**  
Niigata, Japan

**S. GIN**  
Marcoule, France

Abstracted/Indexed in: Aluminium Industry Abstracts/Chemical Abstracts/Current Contents: Engineering, Computing and Technology/Current Contents: Physical, Chemical and Earth Sciences/EI Compendex Plus/Engineered Materials Abstracts/Engineering Index/INSPEC/Metals Abstracts. Also covered in the abstract and citation database Scopus®. Full text available on ScienceDirect®

CONTENTS

EUROFER as wall material: Reduced sputtering yields due to W surface enrichment, <i>J. Roth, K. Sugiyama, V. Alimov, T. Höschen, M. Baldwin and R. Doerner</i>	1	Stoichiometry effect on the irradiation response in the microstructure of zirconium carbides, <i>Y. Yang, W.-Y. Lo, C. Dickerson and T.R. Allen</i>	130
Microstructure stability of candidate stainless steels for Gen-IV SCWR fuel cladding application, <i>J. Li, W. Zheng, S. Penttilä, P. Liu, O.T. Woo and D. Guzunas</i>	7	Surface morphology and deuterium retention in tungsten and tungsten-rhenium alloy exposed to low-energy, high flux D plasma, <i>V.Kh. Alimov, Y. Hatano, K. Sugiyama, M. Balden, M. Oyaidzu, S. Akamaru, K. Tada, H. Kurishita, T. Hayashi and M. Matsuyama</i>	136
Melt processed multiphase ceramic waste forms for nuclear waste immobilization, <i>J. Amoroso, J.C. Marra, M. Tang, Y. Lin, F. Chen, D. Su and K.S. Brinkman</i>	12	Lattice dynamics and lattice thermal conductivity of thorium dicarbide, <i>Z. Liao, P. Huai, W. Qiu, X. Ke, W. Zhang and Z. Zhu</i>	142
Post-irradiation annealing behavior of neutron-irradiated FeCu, FeMnNi and FeMnNiCu model alloys investigated by means of small-angle neutron scattering, <i>F. Bergner, A. Ulbricht, P. Lindner, U. Keiderling and L. Malerba</i>	22	The relationship between microstructure and oxidation effects of selected IG- and NBG-grade nuclear graphites, <i>W.-H. Huang, S.-C. Tsai, C.-W. Yang and J.-J. Kai</i>	149
The formation of radiation-induced segregation at twin bands in ion-irradiated austenitic stainless steel, <i>H.-H. Jin, G.-G. Lee, J. Kwon, S.S. Hwang and C. Shin</i>	28	Redox equilibrium of the $UO_2^{2+}/UO_2^+$ couple in $Li_2MoO_4$ - $Na_2MoO_4$ eutectic melt at 550 °C, <i>T. Nagai, A. Uehara, T. Fujii, N. Sato, H. Kofuji, M. Myochin and H. Yamana</i>	159
Tensile properties and flow behavior analysis of modified 9Cr–1Mo steel clad tube material, <i>K. Singh, S. Latha, M. Nandagopal, M.D. Mathew, K. Laha and T. Jayakumar</i>	37	Two convenient low-temperature routes to single crystals of plutonium dioxide, <i>N.A. Meredith, S. Wang, J. Diwu and T.E. Albrecht-Schmitt</i>	164
Thermophysical characterisation of $ZrC_xN_y$ ceramics fabricated via carbothermic reduction–nitridation, <i>R. Harrison, O. Ridd, D.D. Jayaseelan and W.E. Lee</i>	46	TEM, XRD and nanoindentation characterization of Xenon ion irradiation damage in austenitic stainless steels, <i>H.F. Huang, J.J. Li, D.H. Li, R.D. Liu, G.H. Lei, Q. Huang and L. Yan</i>	168
Post-irradiation induction time in the radiolytic synthesis of $UO_2$ nanoparticles in aqueous solutions, <i>M.C. Ruth and D.B. Naik</i>	54	Evolution of amorphization and nanohardness in SiC under Xe ion irradiation, <i>J. Li, H. Huang, G. Lei, Q. Huang, R. Liu, D. Li and L. Yan</i>	173
Modeling void development in irradiated metals in the phase-field framework, <i>A.A. Semenov and C.H. Woo</i>	60	Redistribution of alloying elements in Zircaloy-2 after in-reactor exposure, <i>G. Sundell, M. Thuvander, P. Tejland, M. Dahlbäck, L. Hallstadius and H.-O. Andrén</i>	178
Thermal measurements and computational simulations of three-phase ( $CeO_2$ - $MgAl_2O_4$ - $CeMgAl_{11}O_{19}$ ) and four-phase (3Y-TZP- $Al_2O_3$ - $MgAl_2O_4$ - $LaPO_4$ ) composites as surrogate inert matrix nuclear fuel, <i>J.P. Angle, A.T. Nelson, D. Men and M.L. Mecartney</i>	69	First-principle study of structural, elastic and electronic properties of Th mononpnictides, <i>S. Amari, S. Mécabihi, B. Abbar and B. Bouhafs</i>	186
First principles calculations predict stable 50 nm nickel ferrite particles in PWR coolant, <i>C.J. O'Brien, Zs. Rák, E.W. Bucholz and D.W. Brenner</i>	77	Depth profile of oxide volume fractions of Zircaloy-2 in high-temperature steam: An <i>in-situ</i> synchrotron radiation study, <i>W. Mohamed, D. Yun, K. Mo, M.J. Pellin, M.C. Billone, J. Almer and A.M. Yacout</i>	192
Thermodynamic re-assessment of the Pu–U system and its application to the ternary Pu–U–Ga system, <i>A. Perron, P.E.A. Turchi, A. Landa, P. Söderlind, B. Ravat, B. Oudot, F. Delaunay and M. Kurata</i>	81	Chemically produced tungsten–praseodymium oxide composite sintered by spark plasma sintering, <i>X.-Y. Ding, L.-M. Luo, Z.-L. Lu, G.-N. Luo, X.-Y. Zhu, J.-G. Cheng and Y.-C. Wu</i>	200
Atomistic simulations of displacement cascades in $Y_2O_3$ single crystal, <i>M. Dholakia, S. Chandra, M.C. Valsakumar and S. Mathi Jaya</i>	96	Interfacial metallurgy study of brazed joints between tungsten and fusion related materials for divertor design, <i>Y. Zhang, A. Galloway, J. Wood, M.B.O. Robbie, D. Easton and W. Zhu</i>	207
An approach to quantifying the chemical conditions necessary to form a magnetite layer on steels in lead and lead–bismuth eutectic, <i>S. Qvist</i>	105	First-principles study of point defects in thorium carbide, <i>D. Pérez Daroca, S. Jaroszewicz, A.M. Llois and H.O. Mosca</i>	217
Influence of TiN nanoparticles on the microstructure and properties of W matrix materials prepared by spark plasma sintering, <i>S. Wang, L.-M. Luo, X.-Y. Tan, G.-N. Luo, X. Zan, J.-G. Cheng, X.-Y. Zhu and Y.-C. Wu</i>	114	Synthesis of lead vanadate iodoapatite utilizing dry mechanochemical process, <i>Y. Suetsugu</i>	223
Effects of Y on helium behavior in Ti–Y alloy films, <i>J. Zhang, E. Wu and S. Liu</i>	119	The use of barytocalcite for carbon 14 immobilization: One-year leaching behavior, <i>N. Massoni, C. Marcou, J. Rosen and P. Jollivet</i>	230
Orientation relationship formed during irradiation induced precipitation of W in Cu, <i>K. Tai, R.S. Averbach, P. Bellon, N. Vo, Y. Ashkenazy and S.J. Dillon</i>	126	In-pile test results of U-silicide or U-nitride coated U-7Mo particle dispersion fuel in Al, <i>Y.S. Kim, J.M. Park, K.H. Lee, B.O. Yoo, H.J. Ryu and B. Ye</i>	238

(Contents continued on inside back cover)



(Contents continued from outside back cover)

Temperature increase of Zircaloy-4 cladding tubes due to plastic heat dissipation during tensile tests at $0.1\text{--}10\text{ s}^{-1}$ strain rates, <i>A. Hellouin de Menibus, Q. Auzoux, J. Besson and J. Crépin</i>	247	Deformation studies from in situ SEM experiments of a reactor pressure vessel steel at room and low temperatures, <i>F. Latourte, T. Salez, A. Guery, N. Rupin and M. Mahé</i>	373
Anisotropic dislocation loop distribution in alloy T91 during irradiation creep, <i>C. Xu and G.S. Was</i>	255	Microstructural changes in a neutron-irradiated Fe-15 at.%Cr alloy, <i>M. Bachhav, G. Robert Odette and E.A. Marquis</i>	381
Tensile deformation behavior and microstructure evolution of Ni-based superalloy 617, <i>D. Kaoumi and K. Hrutkay</i>	265	Iron redistribution in a zirconium alloy after neutron and proton irradiation studied by energy-dispersive X-ray spectroscopy (EDX) using an aberration-corrected (scanning) transmission electron microscope, <i>E.M. Francis, A. Harte, P. Frankel, S.J. Haigh, D. Jädernäs, J. Romero, L. Hallstadius and M. Preuss</i>	387
The effect of temperature on the SSRT behavior of austenitic stainless steels in SCW, <i>Z. Shen, L. Zhang, R. Tang and Q. Zhang</i>	274	Synthesis of dense yttrium-stabilised hafnia pellets for nuclear applications by spark plasma sintering, <i>V. Tyrpekl, M. Holzhäuser, H. Hein, J.-F. Vigier, J. Somers and P. Svora</i>	398
Microstructure changes and thermal conductivity reduction in $\text{UO}_2$ following 3.9 MeV $\text{He}^{2+}$ ion irradiation, <i>J. Pakarinen, M. Khafizov, L. He, C. Wetteland, J. Gan, A.T. Nelson, D.H. Hurley, A. El-Azab and T.R. Allen</i>	283	Characteristics of uranium carbonitride microparticles synthesized using different reaction conditions, <i>C.M. Silva, T.B. Lindemer, S.R. Voit, R.D. Hunt, T.M. Besmann, K.A. Terrani and L.L. Snead</i>	405
Finite element analysis of the tetragonal to monoclinic phase transformation during oxidation of zirconium alloys, <i>P. Platt, P. Frankel, M. Gass, R. Howells and M. Preuss</i>	290	Effect of initial grain size on the hot deformation behavior of 47Zr-45Ti-5Al-3V alloy, <i>Y.B. Tan, L.H. Yang, J.L. Duan, W.C. Liu, J.W. Zhang and R.P. Liu</i>	413
High-temperature heat capacity and density of simulated high-level waste glass, <i>T. Sugawara, J. Katsuki, T. Shiono, S. Yoshida, J. Matsuoka, K. Minami and E. Ochi</i>	298	The behavior of small helium clusters near free surfaces in tungsten, <i>A.V. Barashev, H. Xu and R.E. Stoller</i>	421
First-principles study of the Pd-Si system and Pd(0 0 1)/SiC(0 0 1) hetero-structure, <i>P.E.A. Turchi and V.I. Ivashchenko</i>	308	Master sintering curves for $\text{UO}_2$ and $\text{UO}_2\text{-SiC}$ composite processed by spark plasma sintering, <i>Z. Chen, G. Subhash and J.S. Tulenko</i>	427
Thermal conductivity of porous $\text{UO}_2$ : Molecular Dynamics study, <i>S. Nichenko and D. Staicu</i>	315	Microstructural characterization of irradiated U-7Mo/Al-5Si dispersion fuel to high fission density, <i>J. Gan, B.D. Miller, D.D. Keiser Jr., A.B. Robinson, J.W. Madden, P.G. Medvedev and D.M. Wachs</i>	434
Quantitative TEM analysis of precipitation and grain boundary segregation in neutron irradiated EUROFER 97, <i>C. Dethloff, E. Gaganidze and J. Aktaa</i>	323	First-principles study of water adsorption and dissociation on the $\text{UO}_2$ (1 1 1), (1 1 0) and (1 0 0) surfaces, <i>T. Bo, J.-H. Lan, Y.-L. Zhao, Y.-J. Zhang, C.-H. He, Z.-F. Chai and W.-Q. Shi</i>	446
Corrosion behavior of austenitic steels 1.4970, 316L and 1.4571 in flowing LBE at 450 and 550 °C with $10^{-7}$ mass% dissolved oxygen, <i>V. Tsisar, C. Schroer, O. Wedemeyer, A. Skrypnik and J. Konys</i>	332	Mechanical characterisation of tungsten-1 wt.% yttrium oxide as a function of temperature and atmosphere, <i>T. Palacios, A. Jiménez, A. Muñoz, M.A. Monge, C. Ballesteros and J.Y. Pastor</i>	455
Graphite immobilisation in iron phosphate glass composite materials produced by microwave and conventional sintering routes, <i>M.Z.H. Mayzan, M.C. Stennett, N.C. Hyatt and R.J. Hand</i>	343		
Deformation behavior of laser welds in high temperature oxidation resistant Fe-Cr-Al alloys for fuel cladding applications, <i>K.G. Field, M.N. Gussev, Y. Yamamoto and L.L. Snead</i>	352		
On the shape of stress corrosion cracks in sensitized Type 304 SS in Boiling Water Reactor primary coolant piping at 288 °C, <i>S.-K. Lee, D. Kramer and D.D. Macdonald</i>	359		